
Article:
Pouran, H.M., Banwart, S.A. and Romero-Gonzalez, M. orcid.org/0000-0001-5808-5383 (2017) Effects of synthetic iron and aluminium oxide surface charge and hydrophobicity on the formation of bacterial biofilm. Environmental Science: Processes & Impacts, 19. pp. 622-634. ISSN 2050-7887

https://doi.org/10.1039/C6EM00666C

Effects of synthetic iron and aluminium oxide surface charge and hydrophobicity on the formation of bacterial biofilm

Hamid M. Pouran*[a], Steve A. Banwart[b], Maria Romero-Gonzalez[c]

[a] *LMEI, SOAS, University of London, UK,* [b] *School of Earth and Environment, University of Leeds, UK,* [C] *Department of Geography, University of Sheffield, UK*

*__Corresponding author:__ Dr Hamid M. Pouran: Tel.: +44 (0)7930 342062

Email: hamidpouran@gmail.com

Abstract

In this research, bacterial cell attachments to hematite, goethite and aluminium hydroxide were investigated. The aim was to study the effects of these minerals' hydrophobicity and pH-dependent surface charge on the extent of biofilm formation using six genetically diverse bacterial strains: *Rhodococcus* spp. (RC92 & RC291), *Pseudomonas* spp. (Pse1 & Pse2) and *Sphingomonas* spp. (Sph1 & Sph2), which had been previously isolated from contaminated environments. The surfaces were prepared in a way that was compatible with the naturally occurring coating process in aquifers: deposition of colloidal particles from the aqueous phase. The biofilms were evaluated using a novel, in situ and non-invasive technique developed for this purpose. A manufactured polystyrene 12-well plate was used as the reference surface to be coated with synthesized minerals by deposition of their suspended particles through evaporation.

Planktonic phase growth indicates that it is independent of the surface charge and hydrophobicity of the studied surfaces. The hydrophobic similarities failed to predict biofilm proliferation. Two of the three hydrophilic strains formed extensive biofilms on the minerals. The third one, Sph2, showed anomalies contrary to the expected electrostatic attraction between the minerals and the cell surface. Further research showed how the solution's ionic strength affects Sph2 surface potential and shapes the extent of its biofilm formation; reducing the ionic strength from ≈ 200 mM to ≈ 20 mM led to a tenfold increase in the number of cells attached to hematite. This study provides a technique to evaluate biofilm formation on metal-oxide surfaces, under well-controlled conditions, using a simple yet reliable method. The findings also highlight that cell numbers in the planktonic phase do not necessarily show the extent of cell attachment, and thorough the physicochemical characterization of bacterial strains, substrata and the aquifer medium are fundamental to successfully implementing any bioremediation projects.

Keywords: Interface interactions; Hematite; Goethite; Aluminium hydroxide; Coating; Microorganism; Planktonic growth; Hydrophobicity, Electrostatic interactions; Biofilm formation; Cell adhesion; *Rhodococcus* spp., *Pseudomonas* spp., *Sphingomonas* spp.,

1. Introduction

Biodegradation, utilizing the capability of microorganisms to transform pollutants into new compounds, [1–3] is a key process in planning management strategies for contaminated soils and aquifers. It is known that in a groundwater environment microbial communities form biofilms, which play a predominant role in the biodegradation process. [1,4]

Bacterial adhesion to metal oxides has been a subject of research for many years, either for its positive effect, e.g. its role in bioremediation, or negative impact on industrial process efficiency, e.g. engineering costs because of biofouling (undesirable growth and accumulation of bacterial cells on the surfaces of engineering structures). [5,6] Although understanding biofilm formation requires a multidisciplinary research approach, [6] we often see that this necessity has been undermined when studying bacterial adhesion on mineral surfaces. Available studies on biofilm formation on metal oxides indicate that the dominant technique to prepare these surfaces is often based on precisely engineered methods, e.g. chemical vapour deposition (CVD). [7,8]

This paper aims to provide a better understanding of biofilm formation via the use of some bacterial strains capable of participating in the bioremediation process on the most common metal-oxide surfaces in aquifers. The results will improve our perception of the interfacial forces governing bacterial cell attachment and our ability to speculate on the extent of biofilm formation and consequently biodegradation efficiency in diverse geological media. [1,3,9–11] It is worth mentioning that biofilm formations using selected model strains have been evaluated in other published studies, namely their attached growth on quartz and polystyrene surfaces. [4,9]

Biofilm formation begins with the adhesion of a small quantity of cells. [3,12,13] Figure 1 is a schematic representation of the main steps involved in the biofilm formation process, [13–15] In engineered bioremediation, the traditional assumption is that stimulating a naturally occurring microbial population and/or adding specific microorganisms to a contaminated aquifer will enhance the biodegradation of a targeted compound. [4,14,16] This is based on the concept that deploying these techniques eventually improves biofilm formation and consequently the bioremediation process. For this purpose, planktonic phase growth and variations in cell numbers in this phase are often used to infer bacterial activity, while the success of the bioremediation process depends on effective bacterial colonization and subsequent biofilm formation. [4]

Mineral surface properties can influence both cell attachment and biofilm formation. [4,10,17] The role of surface hydrophobicity and the charge of both the cell surface and the substrate in cell adhesion and attached growth have been studied before and discrepancies between the expected extent of biofilm formation and observed attachment patterns have been found. [4,9,11] This research tests the hypothesis that the surface charge and hydrophobicity of mineral surfaces, specifically metal oxides, determine the extent of biofilm formation. This study differentiates itself from other research by performing tests on metal-oxide surfaces that were synthesized, fully characterized and deposited on reference surfaces in a way compatible with the deposition process that occurs in aquifers, [18–20] e.g. hematite-coated quartz, in contrast to precisely engineered surfaces, e.g. metal-oxide thin films, such as those prepared through chemical vapour deposition (CVD). [10,21,22] Also, this research relies on a novel, in situ and non-invasive technique that uses a water-dipping objective to evaluate biofilm formation on the minerals studied. This imaging method was developed for this

study, and it provides a better way to evaluate and quantify biofilms compared to using crystal violet assay, which is a method frequently used for this purpose. [9]

Metal oxides are an important group of soil minerals, in particular because of their wide presence and the variety of geochemical reactions that occur on their surfaces. [18] Hematite, goethite and aluminium hydroxide are some of the most common soil minerals, they often appear in the form of coatings on other mineral surfaces, such as quartz. [10,19,20] In addition, they have a relatively high point of zero charge (PZC), a specific pH value at which the surface charge is neutral, which makes their surfaces positively charged in the pH range of natural environments. [10,18] These metal oxides were selected as model minerals to evaluate the effects of their surface charge and hydrophobicity on the biofilm formation of specific bacterial strains. Studying these metal oxides also allows building up a more comprehensive picture of how complex surfaces, e.g. aluminosilicates and binary metal oxides, can affect attached microbial growth.

Similar to metal oxides, bacterial cells also carry a pH-dependent surface charge at the cell-water interface. [10,23] This surface charge stems from associated functional groups on the surface of the cell wall, which through protonation/ deprotonation processes generates a pH-dependent surface charge. [24,25] Nevertheless, most of the available information indicates that bacterial surfaces dominantly exhibit an overall negative charge in the pH range of natural environments. [26–29] Hence, attraction between the opposite surface charges of bacterial cell and metal-oxide surfaces with pH values like natural environments is expected. Here, we report the results of studying the biofilm formation of specific environmental isolates on hematite, goethite and aluminium hydroxide, which was performed under well-controlled experimental conditions and in a reproducible manner.

Experimental section

1. Materials and Methods

2.1 Chemicals

In the experiments, certified ACS reagents, chemicals that meet or exceed the latest ACS specifications, were supplied by Fisher Scientific (UK) and used without further purification. Ultra-high quality water (UHQ, conductivity 18.2 MΩ/cm at 25ºC) was used throughout the experiments. All chemicals were prepared in Pyrex glass vessels.

2.2 Surface preparation – synthesis, coating and characterization

Hematite was prepared by heating an acidic solution of $FeCl_3$. [10,30] Goethite was synthesized by heating an alkaline solution of $Fe(NO_3)_3$ in a polyethylene flask for 60 hours at 70°C. [10,31] The aluminium hydroxide synthesis method was based on adding aluminium nitrate to an alkaline solution. [10,32]

A STOE STADI P X-ray powder diffractometer and a Perkin Elmer Spectrum Spotlight FTIR imaging system for Fourier-transform infrared spectroscopy (FTIR) were used to analyze the synthetized materials. For XRD analysis, copper K alfa was the radiation source; a range of 10–70 degrees and a step size of 0.02 degrees were the test parameters. In FTIR experiments, the spectrum resolution was 4 cm^{-1}, covering the range of 4,000-400 cm^{-1} wave numbers, and 150 scans were collected for each sample.

To determine the point of zero charge (PZC) of the synthetic metal oxides, potentiometric titration was done. An automated potentiometric titrator (Metrohm, 718 STAT, Titrino) was used. During titrations, acid (HCl, 0.1M) and base (NaOH, 0.1M) were added by a computer-controlled micro-burette with a dispensing volume of 0.01 ml. The titrator was

adjusted to add successive acid or base when the absolute value of the potential drift was equal to or less than 5 mV/min. The sample suspensions were purged with N_2 gas to remove carbon dioxide from the system for approximately two hours before titration, which was performed in an N_2 atmosphere. [10] In these tests, a magnetic stirrer provided continuous stirring and the suspension temperature was kept at 25ºC during the titration period. Surface hydrophobic/ hydrophilic properties of the synthetic minerals were obtained by measuring the water-drop contact angle in air. Contact angles were obtained using the sessile drop method and a KRÜSS DSA 100 drop-shape analysis system. An aliquote of 3µl of UHQ water was added to the mineral surfaces at room temperature. [10] The contact angle between the surface and a tangent drawn on the drop surface, passing through the triple point of atmosphere-liquid-solid, was measured. Iron and aluminium oxides' hydrophilic nature stems from their surface hydroxyl groups. [33] In general, surfaces with a water-drop contact angle of less than 90 degrees are hydrophilic; nevertheless, for the surfaces studied, the expected water-drop contact angles were considerably less. [34–37] The MATH, Microbial Adhesion to Hydrocarbon Test, is an established method to quantify microbial cell surface hydrophobicity via their attachment to hydrocarbon droplets; [38–40] this technique has been performed on selected model strains in other published studies.

The coating process involved the direct deposition of mineral particles from an aqueous suspension by evaporation, which has been explained in detail in a previous publication. [10] After this step, the coated polystyrene surfaces were assessed using optical microscopy (Zeiss, Axiovision), direct imaging and contact-angle measurements to determine their hydrophobicity (as described above). The ATR-FTIR, attenuated total reflection-Fourier transform infrared, technique using a Specac Silver Gate Essential Single Reflection ATR System and XPS, and X-ray photoelectron spectroscopy (KRATOS-Axis 165) were also used

to compare the chemical properties of altered surfaces with those of reference polystyrene and mineral surfaces[10] – please see supporting information (SI).

2.3 Bacterial strains, growth conditions and sample preparation

Six bacterial strains were isolated for bacterial-adhesion and attached-growth studies. *Rhodococcus* spp., RC92 and RC291, both Gram-positive, were isolated from soil samples from a polluted gasworks site in northeast England. The bacteria *Pseudomonas* spp. (Pse1 and Pse2) and *Sphingomonas* spp. (Sph1 and Sph2) were isolated from groundwater at a phenol-contaminated site in the West Midlands (England). The strains Pse1, Pse2, Sph1 and Sph2 are Gram-negative. They have been classified using comparative 16S rRNA sequencing. [4,9] All strains were maintained on a solid R2A medium (Oxoid). [41]

The bacterial strains were grown in an AB10 medium, [42] which is a defined medium with known exact chemical composition – please see supporting information (SI). The carbon source was 2 mM of glucose, and the incubation time was 96 hours at 20˚C on a shaker at 150 rpm. After incubation, cells were harvested by centrifugation in an early stationary phase and washed in 10 ml of sterile 0.9% NaCl solution. Samples of washed and resuspended strains (in 0.9% NaCl), with an optical density (OD) of 0.01 at λ =600 nm, were resuspended in the AB10 medium with different carbon-source treatments. Two variations of carbon sources, 2 mM of glucose and 2 mM of potassium acetate (KAc), were used to evaluate whether there was a difference between these two carbon sources in the extent of biofilm formation; in addition, the same medium with no carbon source was used as a control. Previous studies indicate that these environmental isolates can metabolize glucose and potassium acetate, and similar growth media have been used in the past to study biofilm formation on model substrata with different surface properties. [4,9] The aim of this study was to perform experiments, including bacterial cell growth and attachment, in a well-controlled environment. A similar incubation method and growth medium (defined medium AB10 [42]), in

addition to studying the attachment morphologies of these individual environmental isolates to polystyrene, have been reported in other publications; [1,4,9–11,43,44] these were used to cross-compare with this research. Extending this study to conditions more compatible with natural environments should be part of future studies.

2.4 Biofilm formation studies

Six strains, four different surfaces, two carbon sources and one experimental control (AB10 medium with no carbon source) were analyzed in triplicate to assay biofilm formation for a total of 216 samples. In these experiments, reference polystyrene plates were prepacked and radiation-sterilized. The mineral-coated polystyrene plates [10] were sterilized by immersion in a 70% ethanol medium for one hour prior to incubation and dried under aseptic conditions in a laminar flow cabinet.

Non-invasive, in situ direct imaging using Syto9 stain (green fluorescent nucleic acid stain, supplied by Invitrogen) was used as the primary technique to assay biofilm. [45,46] The reference polystyrene and metal-oxide coated polystyrene well-plates, each with 12 wells and a nominal culture area of 3.82 cm^2 for each well, [47] were used as substrata for biofilm formation studies. Samples of bacteria suspension were prepared at an optical density (OD) of 0.01 at λ = 600 nm using AB10 medium, pH≈ 6.5, with glucose, potassium acetate and no carbon source. Then, 2 ml of prepared medium was added to each micro-well. The 12 well-plates were incubated for 96 hours at 20°C (Fig. 2); then, 200 µl of each of the bacterial samples, from their planktonic phase, was transferred to a 96-micro well-plate and the OD was measured at λ=630 nm to determine planktonic phase growth. To assess the planktonic phase of individual environmental isolates, the measured optical density (OD) at λ= 630 nm was calibrated against the number of colony-forming units (CFU) for each strain. This calibration was used to compare growth in the planktonic phase for each individual strain.

The rest of the planktonic phase was discarded and each well was gently washed three times by adding 5ml of 0.9% sterile NaCl solution that was slowly added to the well wall and bottom intersection, using a pipette tip, to remove cells in the planktonic phase and ensure that only bacterial cells which had attached to the surface were present.

Each well of the reference polystyrene and coated plates was stained by adding 0.5 ml of Syto 9, which was diluted 500x. The thickness of the added stain layer that formed on the bottom of the well was approximately 1.25 mm (the surface area of each well was 3.82 cm^2). The stained wells were directly imaged in situ using a 100x magnification Zeiss Achroplan water-dipping objective (Fig. 2). For imaging, a Zeiss AxioVision epifluorescence microscope with automated Z-height focusing (Z-stacking) was used for extended depth and field imaging. With this technique a series of images are acquired at different focus positions, which allows imaging through a thick section or of a rough surface (Fig. 2). Images were captured with an Axiocam black & white camera using a 450-490 nm narrow-band pass filter. For each sample, 15 images were captured and then analyzed using AxioVision 4.6 and Image J software. From these digital images, direct cell counts were obtained and reported as cells/cm^2 (since each experiment was conducted in triplicate, each data point represents an average of 45 data points). The microscope water-dipping objective had restricted lateral motion, due to the well's sides, which confined the imaging area (Fig. 2). Images to study bacterial cell attachment on the substrate, at the bottom of each well, were taken from a circular accessible surface with a diameter of 11mm located at the centre of the wells. As mentioned earlier, microscope Z-stacking provided the option of acquiring images at different focus positions. This technique was used to determine biofilm depth when the cells had formed dense biofilms.

3. Results and Discussion

3.1 Surface coating and characterization

XRD and FTIR analysis showed that the synthetic materials matched the expected metal oxides. Detailed surface analysis, including ATR-FTIR, XPS and water-drop contact angle measurements, confirmed the compatibility of the coated reference plate's surface properties with pure mineral phases [10] – please see supporting information (SI) section.

Mineral surfaces' PZC was obtained at the common intersection point of more than one potentiometric titration curve at different ionic strengths. The PZC of polystyrene was considered to be neutral. [4] The PZC for hematite, goethite and aluminum hydroxide was 7.5, 8.5 and 8.9, respectively, indicating a positive charge on the surface at the pH of the adhesion experiments. The contact angle values for polystyrene (90°) and hematite (≈ 45°) demonstrate that both surfaces are hydrophobic. In the case of goethite and aluminium hydroxide, the contact angle value was lower than 10°, indicating that these surfaces are hydrophilic; [10] – for further details and related images please see supporting information (SI) section.

The relative hydrophobicity of the bacterial species studied in this research has been determined before in independent experiments [1,4,9] that suggest that RC92, RC291 and Sph1 are hydrophobic, while Pse1, Pse2 and Sph2 are hydrophilic strains, after incubation in both AB10 with glucose and potassium acetate carbon sources.

The PZC of bacterial cells is typically between 3.5 and 5.0. [5,10,23,24,48] Since the pH of the experiments, approximately 6.5, was higher than the environmental isolates' expected PZC, the overall surface charge of the cells was anticipated to be negative under the experiment's conditions.

With respect to hydrophobicity, RC92, RC291 and Sph1 were hydrophobic, like the reference polystyrene surface, while Pse1, Pse2 and Sph2 were hydrophilic, similar to the hematite, goethite and aluminium hydroxide coated well-plates. Considering electrostatic

interactions, the PZC values of the bacterial strains and the metal oxide surfaces were, respectively, below and above the experiments' pH (6.5); therefore, electrostatic attraction was expected to drive cell adhesion and subsequent biofilm growth on the mineral surfaces.

3.2 Biofilm studies

Figure 3. shows the total number of cells calculated in the planktonic phase for the studied strains and surfaces. These data relate to the growth medium, AB10, when glucose was the carbon source. As seen in the planktonic phase cell numbers, for each strain, these were within the same range and compatible, regardless of the study surface. Similar patterns were observed when the AB10 carbon source was potassium acetate (KAc) – please see supporting information (SI). The bacterial strains did not grow on the AB10 medium with no added carbon source. The results suggest that the strains thrive better in a medium with a glucose carbon source compared to potassium acetate. More importantly, the level of cell growth in the planktonic phase seems to be independent of the surface charge and hydrophobicity of the growing environment's surface. As Figure 3 indicates, the numbers of RC92 and RC291, *Rhodococcus* spp., in the planktonic phase are less than *Pseudomonas* spp. (Pse1 & Pse2), and *Sphingomonas* spp. (Sph1 & Sph2). This can be attributed to the surface properties of the *Rhodococcus* species that encourage cell aggregation in an aqueous medium. [49,50] Prior to measuring the planktonic phase, the samples were vortexed to disperse flocs of these strains.

Based on the hydrophobic properties of the cells and surfaces, the expected pattern is to see more cell attachment of the hydrophobic strains, RC92, RC91 and Sph1, on polystyrene, and more biofilm on the hydrophilic reference mineral surfaces formed by Pse1, Pse2 and Sph2.

Figures 4–6 show the bacterial strain adhesion patterns of the reference polystyrene and mineral surfaces in the AB10 medium with a glucose carbon source. The biofilms formed on polystyrene are similar to those previously reported in other research, using the same variables. [4,9]

RC92 had overall poor attachment on the studied surfaces. The attached growth colonies of this strain on the reference polystyrene formed different groups of cells that aligned to shape and split and relatively short chain-type cell arrangements, while for the mineral surfaces attached individual and separated cells were observed (Figs 4a–4d). RC291 is a Gram-positive, hydrophobic bacterial strain like RC92, with comparable attachment morphologies for minerals, but different colony forms on the reference polystyrene surface. As shown in Figure 4h, RC291 forms proliferated, with dense and highly structured biofilm on the reference polystyrene.

Pse1 and Pse2 are Gram-negative and hydrophilic. As seen in Figure 5 (a–d), Pse1 forms cell clusters on all surfaces; however, the numbers and sizes of these clusters are considerably higher for biofilms attached to metal oxides. The biofilms on polystyrene are sparse and shape small micro-colonies (Fig. 5d), while they are notably denser on mineral surfaces. Pse2 shows the same biofilm formation phenotype on metal oxides, Figure 5 (e–g), but for the polystyrene the attached cells are more aggregated and show discrete micro-colonies (Fig. 5h).

In these experiments, Sph1 was the only Gram-negative strain with hydrophobic surface properties. As Figure 6 (a–c) displays, Sph1 cells attached to mineral surfaces show poor adhesion, while biofilms formed on reference polystyrene are extensive and abundant (Fig. 6d). Sph2 is a Gram-negative strain with hydrophilic surface properties. Negligible attachment to metal oxide surfaces (Fig. 6 e–g), in contrast to the notable biofilm formation on reference polystyrene, compatible with Sph1, was the dominant morphology for attached

cells. The results are striking, as hydrophobic Sph1 and hydrophilic Sph2 show matching biofilm formation patterns on the studied surfaces. Table 1 summarizes the biofilm morphologies of attached cells on the studied mineral and polystyrene surfaces.

The observed morphologies for attached cells using KAc as the carbon source were similar to AB10 with glucose – please supporting information (SI) for details.

Figure 7 shows the numbers of attached cells based on a direct count of cell numbers from captured images. As seen, Pse1 and Pse2 are the strains with the highest numbers of attached cells to metal oxides. The cell numbers for RC92 and RC291 are significantly higher for the reference polystyrene compared to mineral surfaces. Similarly, the numbers of Sph1 and Sph2 attached cells are notably higher for the reference polystyrene compared to the metal oxides.

Comparing the numbers of attached cells on the studied surfaces (Fig. 7) with their respective planktonic phase growth (Fig. 3) suggests that a high number of cells in the planktonic phase does not necessarily correspond to extensive cell attachment and biofilm formation.

The hydrophobic nature of the *Rhodococcus* strains, RC92 and RC291, is a likely reason for their negligible attachment to hydrophilic minerals. Nevertheless, hydrophobicity does not fully explain their attachment pattern to the hydrophobic reference polystyrene surface and the clear differences in biofilm morphology seen between these two strains (Figs 6 d, h). A previous study [4] suggests that lipophilic macromolecules of RC92 and RC291 cell walls play a key role in their attachment to hydrophobic polystyrene surfaces. These macromolecules associate differently with cells, which consequently influences cell attachment and biofilm proliferation on hydrophobic surfaces. For RC291, polar and non-polar lipids are closely associated with the cells that facilitate cell attachment to hydrophobic surfaces and cell-cell interactions. In contrast, although RC92 produces large numbers of

diverse extracellular lipophilic molecules, these materials are not closely associated with the cells and can be detached and released to the medium. Therefore, the ability to retain extracellular lipophilic materials is a likely element that shapes the attachment phenotypes of RC92 and RC291. [4]

Pse1 and Pse2, despite similarities in their genetics, attach differently to polystyrene. They show similar attachment morphologies, but the number of cells attached to the polystyrene surface is notably higher for Pse1. The difference in the extent of attachment to the studied surfaces, and the considerable biofilm formation of these hydrophilic strains on the hydrophobic polystyrene surface, can be attributed to their specific physiological features. [51] Other studies, [4,44] using microscopic and spectroscopic analyses in addition to studying cell attachments under treatment with D-Nasel, have revealed that for the *Pseudomonas* species the extracellular DNA (eDNA) determines the difference between Pse1 and Pse2 attachment patterns. The presence of eDNA enhances Pse1 adhesion to a hydrophobic surface.

The *Sphingomonas* strains' adhesion patterns to hydrophobic polystyrene and hydrophilic mineral surfaces are compatible. The *Sphingomonas* species has Gram-negative strains, these are unique compared to other Gram-negatives. Instead of lipopolysaccharide (LPS) *Sphingomonaceae spp.,* bacterial strains have glycosphingolipids (GSL), which are a subgroup of glycolipids (lipids that are linked to a carbohydrate chain). They contain the sphingosine, an amino alcohol, moiety. These chemical structures are amphiphilic, having both hydrophobic and hydrophilic parts, the molecules generally have similarities to the physicochemical and functional properties of lipopolysaccharides. [52,53] The amphiphilic characteristi of these *Sphingomonas spp*. Cell-surface molecules can probably facilitate the attachment of these strains to both hydrophobic and hydrophilic surfaces. Similar biofilm formation patterns of Sph2 on a polystyrene surface have been reported before. [4,9] However, this characteristic does not explain the poor Sph2 attachment to mineral surfaces. The

polystyrene surface charge is neutral, [10] so electrostatic interactions can only play a negligible role in Sph2 attachment to this surface. Unlike hydrophobic polystyrene, mineral surfaces are hydrophilic with a positive surface charge [10] in pH of the experiment. The expected PZC of Sph2 under the experimental condition, pH 6.5, is negative and attractive cell-mineral electrostatic interaction is anticipated to support cell attachment and biofilm formation. This is contrary to the observed pattern. To investigate these discrepancies further, additional experiments were performed to determine if medium ionic strength affects the electrostatic interactions between two hydrophilic entities.

Sph2 zeta potential was measured using a zeta potential analyzer (Zeta Plus, Brookhaven Instruments, Huntsville, NY). Zeta potential can be defined as the electrical potential difference when there is interference between a bulk aqueous medium and a static fluid attached to a bacterial cell. [54]

Figure 8a shows zeta potential values for a Sph2 strain suspended in 1 mM of KCl. As can be seen, this bacterial strain shows negative surface potential at circa neutral pH values. This agrees with previously published research indicating that bacterial cells often have a relatively low PZC and carry a negative surface charge in natural media. [5,10,23,24,48] Nevertheless, this result cannot explain the attachment behaviour of Sph2 on positively charged metal-oxide surfaces.

In this research, cell attachments were evaluated after 96 hours of incubation. During this time, bacterial cells, immersed in an AB10 medium, were exposed to metal oxides and polystyrene surfaces. To evaluate the effect of incubation time on cell surface charge, Sph2 cells were harvested from the planktonic phase of hematite plates at the end of incubation and their PZC were measured in 1mM of KCl (pH ≈ 6.5). The result was consistent with previous zeta potential measurement and was approximately -20±3mV. This test could not be

successfully performed for cells attached to a hematite surface as sampling these cells was not feasible without removing the hematite coating deposited.

The AB10 medium is relatively high in ionic content and has an ionic strength (IS) value of 196.08 mM. Different studies show that increasing ionic strength leads to shrinkage of the diffuse double layer length around a charged colloidal particle, consequently hampering the effects of electrostatic interaction within a specific distance from the surface. Chen and Walker (2007) [54] showed that changing the ionic strength from 1 mM to 100 mM using KCl as the electrolyte caused considerable changes in bacterial cell surface potential. Considering this possibility, the zeta potential of Sph2 (planktonic) was measured in a suspension of AB10 medium with lower levels of ionic strength. NaCl has the highest concentration in this medium (please see supporting information (SI)), and reducing the original ionic strength, from 196.08mM to 98.8 mM and 19.06mM, was achieved by changing this electrolyte concentration in the AB10.

The results of this experiment are shown in Figure 8b. As seen, there was an approximately 20 mV difference between the measured zeta potential for a cell suspension in AB10 medium (identical to the attached growth experimental conditions) and an Sph2 cell suspension in 1mM of KCl. The cell surface charge was less negative and close to zero in the AB10 medium compared to 1mM of KCl. This result may explain the notable attachment of Sph2 to the polystyrene surface. The attraction forces due to electrostatic interactions might have made a negligible contribution to attachment, since the surface charge of the polystyrene and the effective surface charge of the bacterial strain were close to zero under the experiment's conditions. Therefore, attachment was probably governed by hydrophobicity. This case is supported by the fact that the outer cell-wall components of Sph2 are amphiphilic in nature, and this allows bacterial cells to attach and form a biofilm on a hydrophobic surface. This might also have been reinforced by the complexation of the charged groups on

the outer cell wall macromolecules, due to the presence of positively charged ions in the AB10, leading to conformational changes in the macromolecules. As a result, hydrophobic moieties might be more exposed to the ambient environment and facilitate adhesion to a hydrophobic surface.

This finding underlines the role of the growth medium's ionic strength. It also sheds light on the anomalies observed when studying Sph2 attachment to minerals and why cell-adhesion patterns are not consistent with the expected electrostatic attraction that should exist between Sph2 and metal-oxide surfaces. Considering the aforementioned facts, changing the ionic strength and consequently Sph2 surface potential should lead to different attachment behaviour. Reducing the ionic strength and altering the Sph2 surface potential (from close to neutral to ≈ -20mV) should cause a considerable increase in the number of cells attaching to positively charged metal oxides. Figure 9 shows the biofilm formation of Sph2 on a hematite surface in three different ionic strength conditions (pH = 6.5). Figure 10 shows the numbers of Sph2 cells attached to a hematite surface after 96 hours of incubation at three different ionic strengths. As can be seen, when the ionic strength was reduced by a factor of ten, the number of the cells attached to the hematite increased approximately tenfold. The difference in Sph2 surface potential under these two conditions is approximately -20mV, which reinforces the electrostatic attraction between positively charged hematite and a negatively charged Sph2 surface.

In this research, biofilm formations on synthetic mineral surfaces of iron and aluminium oxides were studied under controlled laboratory conditions. The coating method, deposition of metal oxide colloidal particles from a suspension onto a cell-culture polystyrene surface, proved to be a simple but reliable approach for this purpose. This technique can be used in future studies to create multi-component surfaces that better represent the complexity of available mineral surfaces in nature. The novel imaging method developed for this

research also indicates that direct, non-invasive and in situ imaging using a water-dipping objective and Syto9 stain is a good alternative to crystal violet assay that is frequently used for studying biofilm formation.

The planktonic phase of environmental isolates suggest that these were not affected by the surface properties of hematite, goethite, aluminium hydroxide or model polystyrene. Planktonic-phase growth was better in the medium with a glucose-carbon source treatment compared to potassium acetate.

The experimental results suggest that cell-adhesion predictions based on the effects of electrostatic and hydrophobic interactions are likely to show discrepancies when compared to real attachment behaviour. In natural environments, the available surfaces for cell adhesion and biofilm formation, and the bacterial cell surface itself, are not pristine but affected by the ionic composition of the media, e.g. marine and groundwater environments. The dramatic increase in the number of Sph2 attached cells to the hematite surface, by changing the solution ionic strength, is a prime example of this effect; reducing the growth medium's ionic strength from ≈ 200 mM to ≈ 20 mM resulted in ten times more attached cells

This research also demonstrates that the presence of a high number of bacterial cells in the planktonic phase does not necessarily represent extensive cell attachment and biofilm formation on surfaces. This finding is significant because in engineered bioremediation a high number of bacterial cells in the planktonic phase is often considered to be a good indication of the extent of biofilm formation in aquifers. The results suggest that when engineered solutions are planned, realistic predictions of bioremediation are only possible if the physicochemical properties of bacterial cells and mineral surfaces and the ionic strength of aquifer media are thoroughly characterized.

Supporting information

Supplementary data associated with this article can be found in the online version. Potentiometric titration of synthetic minerals, water-drop contact-angle measurements and XRD and FTIR spectra of synthetic minerals are available in this section. In addition, XPS spectra of the reference polystyrene and metal-oxide coated surfaces, details of the AB10 growth medium's ionic content, the planktonic growth and biofilm formation of RC92, RC291, Pse1, Pse2, Sph1 and Sph2 bacterial strains when incubated under a KAc carbon source treatment are provided.

References

(1) Elliott, D. R.; Scholes, J. D.; Thornton, S. F.; Rizoulis, A.; Banwart, S. A.; Rolfe, S. A. Dynamic changes in microbial community structure and function in phenol-degrading microcosms inoculated with cells from a contaminated aquifer. *FEMS Microbiol Ecol* **2010**, *71* (2), 247–259.

(2) Fingerman, M. *Bioremediation of aquatic and terrestrial ecosystems*; CRC Press, 2016.

(3) Kanematsu, H.; Barry, D. M. Environmental Problems: Soil and Underground Water Treatment and Bioremediation. In *Biofilm and Materials Science*; Springer International Publishing: Cham, 2015; pp 117–123.

(4) Andrews, J. S.; Rolfe, S. A.; Huang, W. E.; Scholes, J. D.; Banwart, S. A. Biofilm formation in environmental bacteria is influenced by different macromolecules depending on genus and species. *Environ. Microbiol.* **2010**, *12*, 2496–2507.

(5) Ojeda, J. J.; Romero-Gonzalez, M. E.; Bachmann, R. T.; Edyvean, R. G. J.; Banwart, S. A.; Building, F. M.; Uni, T.; Street, M.; Sheffield, S.; Kingdom, U. Characterization of the cell surface and cell wall chemistry of drinking water bacteria by combining XPS, FTIR spectroscopy, modeling, and potentiometric titrations. *Langmuir* **2008**, *24* (8), 4032–4040.

(6) Karunakaran, E.; Mukherjee, J.; Ramalingam, B.; Biggs, C. A. "Biofilmology": a multidisciplinary review of the study of microbial biofilms. *Appl. Microbiol. Biotechnol.* **2011**, *90* (6), 1869–1881.

(7) Salerno, M. B.; Logan, B. E.; Velegol, D. Importance of molecular details in predicting bacterial adhesion to hydrophobic surfaces. *Langmuir* **2004**, *20*, 10625–10629.

(8) Kwon, K. D.; Vadillo-Rodriguez, V.; Logan, B. E.; Kubicki, J. D. Interactions of biopolymers with silica surfaces: Force measurements and electronic structure calculation studies. *Geochim. Cosmochim. Acta* **2006**, *70*, 3803–3819.

(9) Geoghegan, M.; Andrews, J. S.; Biggs, C. A.; Eboigbodin, K. E.; Elliott, D. R.; Rolfe, S.; Scholes, J.; Ojeda, J. J.; Romero-Gonzalez, M. E.; Edyvean, R. G. J.; et al. The polymer physics and chemistry of microbial cell attachment and adhesion. *Faraday Discuss* **2008**, *139*, 28-85-420.

(10) Pouran, H. M.; Banwart, S. a.; Romero-Gonzales, M.; Romero-Gonzalez, M.; Romero-Gonzales, M. Coating a polystyrene well-plate surface with synthetic hematite, goethite and aluminium hydroxide for cell mineral adhesion studies in a controlled environment. *Appl. Geochemistry* **2014**, *42* (1986), 60–68.

(11) Rizoulis, A.; Elliott, D. R.; Rolfe, S. A.; Thornton, S. F.; Banwart, S. A.; Pickup, R. W.; Scholes, J. D. Diversity of planktonic and attached bacterial communities in a phenol-contaminated sandstone aquifer. *Microb Ecol* **2013**, *66* (1), 84–95.
(12) Crawford, R.; Webb, H.; Truong, V.; Hasan, J. Surface topographical factors influencing bacterial attachment. *Adv. colloid* **2012**.
(13) Zhang, X.; Zhang, Q.; Yan, T.; Jiang, Z. Quantitatively Predicting Bacterial Adhesion Using Surface Free Energy Determined with a Spectrophotometric Method. *Sci. Technol.* **2015**.
(14) Lyon, D.; Vogel, T. Bioaugmentation for groundwater remediation: an overview. *Bioaugmentation Groundw. Remediat.* **2013**.
(15) Scow, K. M.; Hicks, K. A. Natural attenuation and enhanced bioremediation of organic contaminants in groundwater. *Curr Opin Biotechnol* **2005**, *16* (3), 246–253.
(16) Shephard, J. J.; Savory, D. M.; Bremer, P. J.; McQuillan, A. J. Salt Modulates Bacterial Hydrophobicity and Charge Properties Influencing Adhesion of Pseudomonas aeruginosa (PA01) in Aqueous Suspensions. *Langmuir* **2010**, *26*, 8659–8665.
(17) and, L.-C. X.; Logan*, B. E. Interaction Forces Measured Using AFM between Colloids and Surfaces Coated with Both Dextran and Protein. **2006**.
(18) Stumm, W.; Morgan, J. J. Aquatic chemistry, chemical equilibria and rates in natural waters. **1996**.
(19) Dixon, J. B.; Weed, S. B. Minerals in Soil Environment. *SSSA B. Ser.* **1992**.
(20) Huang, P. M.; Li, Y.; Sumner, M. E. (Malcolm E. . *Handbook of soil sciences : properties and processes*; CRC Press, 2012.
(21) Li, B.; Logan, B. E. Bacterial adhesion to glass and metal-oxide surfaces. **2004**, *36*, 81–90.
(22) Moradi, M.; Song, Z.; Nie, X.; Yan, M.; Hu, F. Q. Investigation of bacterial attachment and biofilm formation of two different Pseudoalteromonas species: Comparison of different methods. *Int. J. Adhes. Adhes.* **2016**, *65*, 70–78.
(23) Ojeda, J. J.; Romero-Gonzalez, M. E.; Pouran, H. M.; Banwart, S. a.; Romero-Gonzales, M. E.; Lane, B. In situ monitoring of the biofilm formation of Pseudomonas putida on hematite using flow-cell ATR-FTIR spectroscopy to investigate the formation of inner-sphere bonds between the bacteria and the mineral. *Mineral. Mag.* **2008**, *72* (1), 101–106.
(24) Claessens, J.; van Lith, Y.; Laverman, A. M.; Van Cappellen, P. Acid-base activity of live bacteria: Implications for quantifying cell wall charge. *Geochim. Cosmochim. Acta* **2006**, *70*, 267–276.
(25) Lalonde, S. V; Smith, D. S.; Owttrim, G. W.; Konhauser, K. O. Acid-base properties of cyanobacterial surfaces I: Influences of growth phase and nitrogen metabolism on cell surface reactivity. *Geochim. Cosmochim. Acta* **2008**, *72*, 1257–1268.
(26) Yee, N.; Benning, L. G.; Phoenix, V. R.; Ferris, F. G. Characterization of metal-cyanobacteria sorption reactions: A combined macroscopic and infrared spectroscopic investigation. *Env. Sci Technol* **2004**, *38*, 775–782.
(27) Vijayaraghavan, K.; Yun, Y. S. Bacterial biosorbents and biosorption. *Biotechnol. Adv.* **2008**, *26*, 266–291.
(28) Kapetas, L.; Ngwenya, B. T.; Macdonald, A. M.; Elphick, S. C. Kinetics of bacterial potentiometric titrations: The effect of equilibration time on buffering capacity of Pantoea agglomerans suspensions. *J. Colloid Interface Sci.* **2011**, *359*, 481–486.
(29) French, S.; Puddephatt, D.; Habash, M.; Glasauer, S. The dynamic nature of bacterial surfaces: Implications for metal–membrane interaction. *Crit. Rev. Microbiol.* **2013**, *39* (2), 196–217.
(30) Penners, N. H. G.; Koopal, L. K. Preparation And Optical-Properties Of Homodisperse Hematite Hydrosols. *Colloids And Surfaces* **1986**, *19*, 337–349.
(31) Schwertmann, U.; Cornell, R. M.; Wiley InterScience (Online service). *Iron oxides in the laboratory : preparation and characterization*; Wiley-VCH, 2008.
(32) Tang, B.; Ge, J. C.; Zhuo, L. H.; Wang, G. L.; Niu, J. Y.; Shi, Z. Q.; Dong, Y. B. A facile and controllable synthesis of gamma-Al2O3 nanostructures without a surfactant. *Eur. J. Inorg. Chem.* **2005**, 4366–4369.
(33) Cornell, R. M.; Schwertmann, U. The Iron Oxides: Structure, Properties, Reactions, Occurrences and UsesSecond, Completely Revised and Extended Edition. **2003**.
(34) Costanzo, P. M.; Wu, W.; Giese, R. F.; Vanoss, C. J. Comparison Between Direct-Contact

Angle Measurements And Thin-Layer Wicking On Synthetic Monosized Cuboid Hematite Particles. *Langmuir* **1995**, *11*, 1827–1830.
(35) Costanzo, P. M.; Wu, W.; Giese, R. F. Comparison between Direct Contact Angle Measurements and Thin Layer Wicking on Synthetic Monosized Cuboid Hematite Particles. **1996**, No. 7, 1827–1830.
(36) Lu, H. B.; Liao, L.; Li, J. C.; Shuai, M.; Liu, Y. L. Hematite nanochain networks: Simple synthesis, magnetic properties, and surface wettability. *Appl. Phys. Lett.* **2008**, *92*, 19–21.
(37) Förch, R.; Schönherr, H.; Jenkins, A. T. A. *Surface design : applications in bioscience and nanotechnology*; Wiley-VCH, 2009.
(38) Rosenberg, M.; Gutnick, D.; Rosenberg, E. Adherence Of Bacteria To Hydrocarbons - A Simple Method For Measuring Cell-Surface Hydrophobicity. *Fems Microbiol. Lett.* **1980**, *9*, 29–33.
(39) Busscher, H. J.; Belt-Gritter, B. van de; Mei, H. C. van der. Implications of microbial adhesion to hydrocarbons for evaluating cell surface hydrophobicity - 1. Zeta potentials of hydrocarbon droplets. *Colloids Surfaces B Biointerfaces* **1995**, *3–4* (5), 111–116.
(40) Pablos, C.; van Grieken, R.; Marugán, J.; Chowdhury, I.; Walker, S. L. Study of bacterial adhesion onto immobilized TiO2: Effect on the photocatalytic activity for disinfection applications. *Catal. Today* **2013**, *209*, 140–146.
(41) CM0906, R2A Agar | Oxoid - Product Detail http://www.oxoid.com/UK/blue/prod_detail/prod_detail.asp?pr=CM0906.
(42) Tolker-nielsen, T. I. M.; Brinch, U. C.; Ragas, P. C.; Andersen, J. B. O.; Jacobsen, C. S.; Molin, S. Development and dynamics of Pseudomonas sp biofilms. *J. Bacteriol.* **2000**, *182* (22), 6482–6489.
(43) Elliott, D. R.; Scholes, J. D.; Thornton, S. F.; Rizoulis, A.; Banwart, S. A.; Rolfe, S. A. Dynamic changes in microbial community structure and function in phenol-degrading microcosms inoculated with cells from a contaminated aquifer. *FEMS Microbiol. Ecol.* **2009**, *71* (2).
(44) Andrews, J. S.; Pouran, H. M.; Scholes, J.; Rolfe, S. A.; Banwart, S. A. Multi-factorial analysis of surface interactions in single species environmental bacteria and model surfaces. *Geochim. Cosmochim. Acta* **2009**, *73*, A44–A44.
(45) Acid, N.; Sampler, S. SYTO ® Green-Fluorescent Nucleic Acid Stains. **2008**, *33342*, 1–7.
(46) Suwarno, S. R.; Hanada, S.; Chong, T. H.; Goto, S.; Henmi, M.; Fane, A. G. The effect of different surface conditioning layers on bacterial adhesion on reverse osmosis membranes. *Desalination* **2016**, *387*, 1–13.
(47) Falcon Polystyrene Microplates 12-well; Standard tissue culture; Flat-bottom; https://www.fishersci.com/shop/products/falcon-tissue-culture-plates-12-well-standard-tissue-culture-flat-bottom-growth-area-3-8cm2-well-volume-6ml-1-tray/0877229.
(48) Leone, L.; Ferri, D.; Manfredi, C.; Persson, P.; Shchukarev, A.; Sjoberg, S.; Loring, J. Modeling the acid-base properties of bacterial surfaces: A combined spectroscopic and potentiometric study of the gram-positive bacterium Bacillus subtilis. *Env. Sci Technol* **2007**, *41*, 6465–6471.
(49) Bouchez-Naitali, M.; Vandecasteele, J. P.; Vandecasteele, Æ. J.; Bouchez-naı, M. Biosurfactants, an help in the biodegradation of hexadecane? The case of Rhodococcus and Pseudomonas strains. *World J. Microbiol. Biotechnol.* **2008**, *24*, 1901–1907.
(50) Bouchez-naı, M.; Blanchet, D.; Bouchez-Naitali, M.; Blanchet, D.; Bardin, V.; Vandecasteele, J. P. Evidence for interfacial uptake in hexadecane degradation by Rhodococcus equi: the importance of cell flocculation. *Microbiology-Sgm* **2001**, *147*, 2537–2543.
(51) Huang, W.; Andrews, J.; Wang, Y. Ultrasonic DNA Transfer to Gram-Negative and Gram-Positive Bacteria. *Abstr. Gen. Meet. Am. Soc. Microbiol.* **2008**, *108*, 548.
(52) Kawahara, K.; Moll, H.; Knirel, Y. A.; Seydel, U.; Zahringer, U. Structural analysis of two glycosphingolipids from the lipopolysaccharide-lacking bacterium Sphingomonas capsulata. *Eur. J. Biochem.* **2000**, *267*, 1837–1846.
(53) Pruett, S. T.; Bushnev, A.; Hagedorn, K.; Adiga, M.; Haynes, C. A.; Sullards, M. C.; Liotta, D. C.; Merrill, A. H. Biodiversity of sphingoid bases ("sphingosines") and related amino alcohols. *J. Lipid Res.* **2008**, *49* (8), 1621–1639.

(54) Chen, G. X.; Walker, S. L. Role of solution chemistry and ion valence on the adhesion kinetics of groundwater and marine bacteria. *Langmuir* **2007**, *23*, 7162–7169.

Legends to Figures

Figure 1. Schematic representation of the main mechanisms involved in biofilm formation.

Figure 2. Schematic representation of incubating polystyrene and mineral-coated 12-well plates and directly imaging the strains attached to the studied surfaces. (a) Depicts confined lateral movements of the water-dipping objective due to the well's sides. As seen, a circle of diameter 11 mm located at the centre of each well's base was imaged for the studied substrata. (b) Shows direct imaging of the aluminium hydroxide-coated plates. (c) Illustrates the function of Z-height focusing, Z stacking, used in evaluating biofilm formation. This method was used for dense biofilms to better assess the numbers of cells attached to polystyrene and mineral surfaces.

Figure 3. Total numbers of cells in the planktonic phase for mineral-coated and reference polystyrene plates after 96 hours of incubation in AB10 medium with a glucose carbon source.

Figure 4. RC92 and RC291 attachments to mineral and polystyrene surfaces, a–d refer to RC92 and e–h refer to RC291 adhesion to hematite, goethite, aluminium hydroxide and polystyrene, respectively (AB10 medium with glucose carbon sources, ionic strength = 196.08mM, pH= 6.5).

Figure 5. Pse1 and Pse2 attachment to mineral and polystyrene surfaces, a–d refer to Pse1 and e–h refer to Pse2 adhesion to hematite, goethite, aluminium hydroxide and polystyrene, respectively (AB10 medium with glucose carbon sources, ionic strength = 196.08mM, pH= 6.5).

Figure 6. Sph1 and Sph2 attachment to mineral and polystyrene surfaces, a-d refer to Sph1 and e-h refer to Sph2 adhesion to hematite, goethite, aluminium hydroxide and polystyrene, respectively (AB10 medium with glucose carbon sources, ionic strength = 196.08mM, pH= 6.5).

Figure 7. Total number of bacterial cells attached to mineral-coated polystyrene and polystyrene surfaces after 96 hours of incubation in AB10 medium with a glucose carbon source.

Figure 8. (a) Zeta potential of Sph2 strain suspended in 1 mM of KCl at different pH values. (b). Variations of the zeta potential of Sph2 strain in AB10 medium at different ionic strengths.

Figure 9. Attachment of Sph2 to a hematite surface under different ionic strengths (a; IS =196.08 mM, b; IS = 98.08 mM, c; IS = 19.06 mM).

Figure 10. Quantified number of cells attached to hematite after 96 hours of incubation under different ionic strength (IS) conditions.

Table 1. Summarizes bacterial strains; RC92, RC291, Pse1, Pse2, Sph1 and Sph2 adhesion morphologies to polystyrene and mineral surfaces.

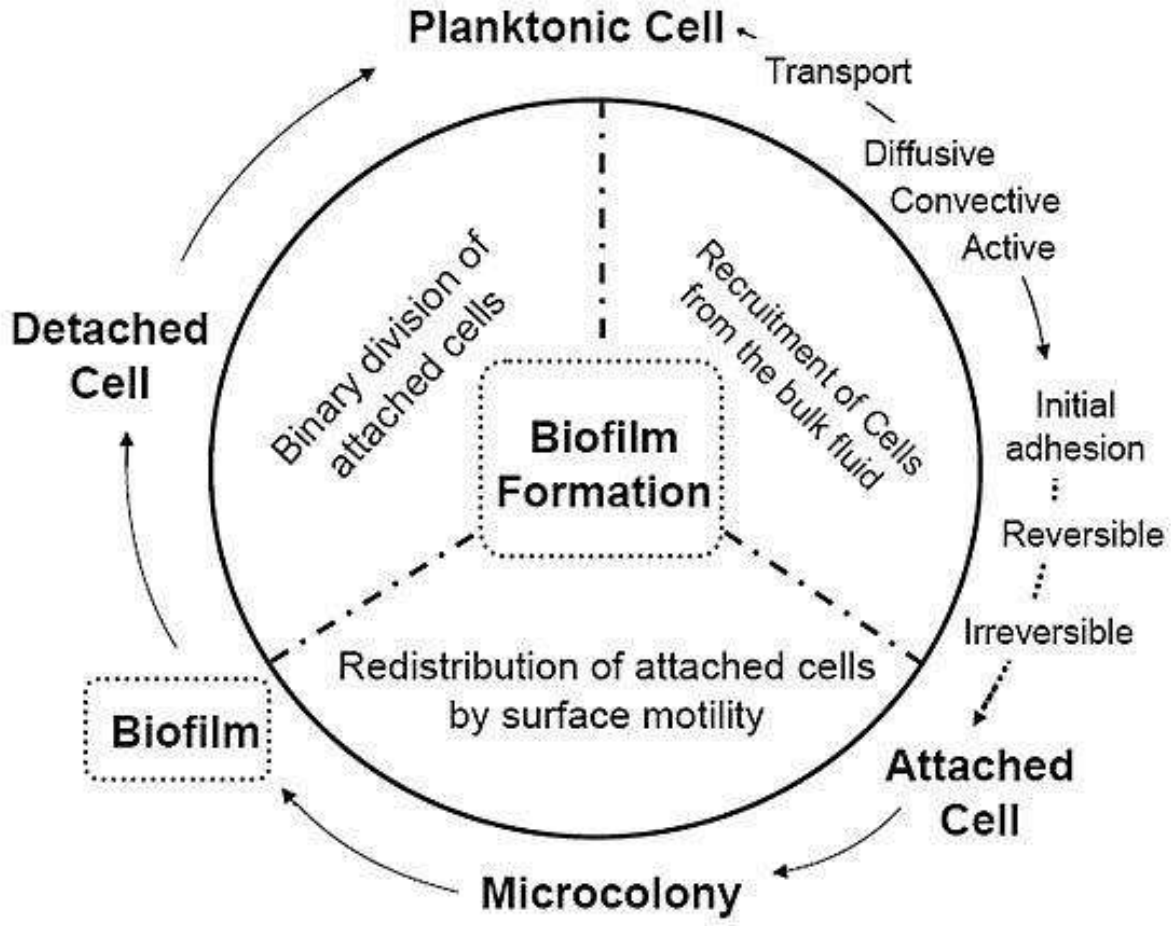

Figure 1

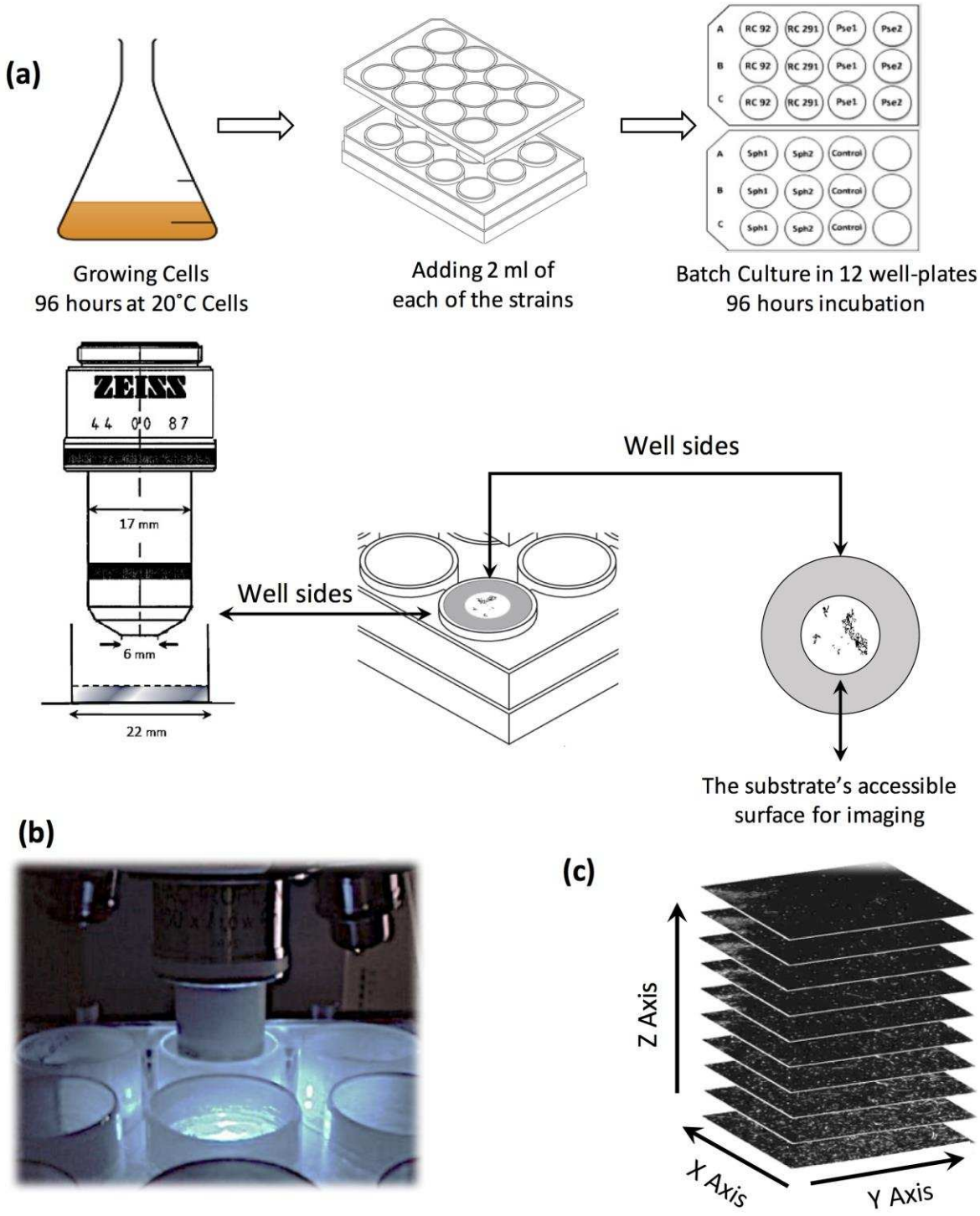
(a)
Growing Cells
96 hours at 20˚C Cells
Adding 2 ml of
each of the strains
Batch Culture in 12 well-plates
96 hours incubation
RC 92
RC 291
Pse1
Pse2
Sph1
Sph2
Control
ZEISS
17 mm
6 mm
22 mm
Well sides
Well sides
The substrate's accessible
surface for imaging
(b)
(c)
Z Axis
X Axis
Y Axis

Figure 2

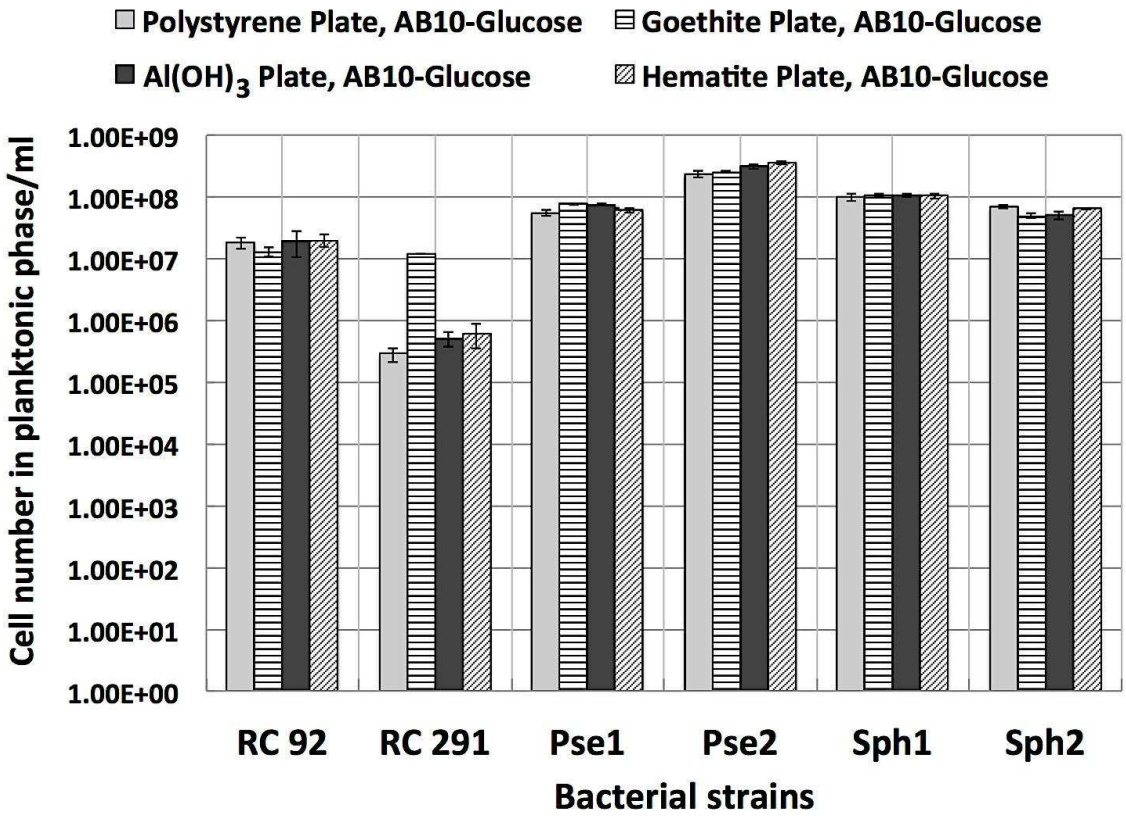
Polystyrene Plate, AB10-Glucose
Goethite Plate, AB10-Glucose
Al(OH)3 Plate, AB10-Glucose
Hematite Plate, AB10-Glucose
Cell number in planktonic phase/ml
1.00E+09
1.00E+08
1.00E+07
1.00E+06
1.00E+05
1.00E+04
1.00E+03
1.00E+02
1.00E+01
1.00E+00
RC 92
RC 291
Pse1
Pse2
Sph1
Sph2
Bacterial strains

Figure 3

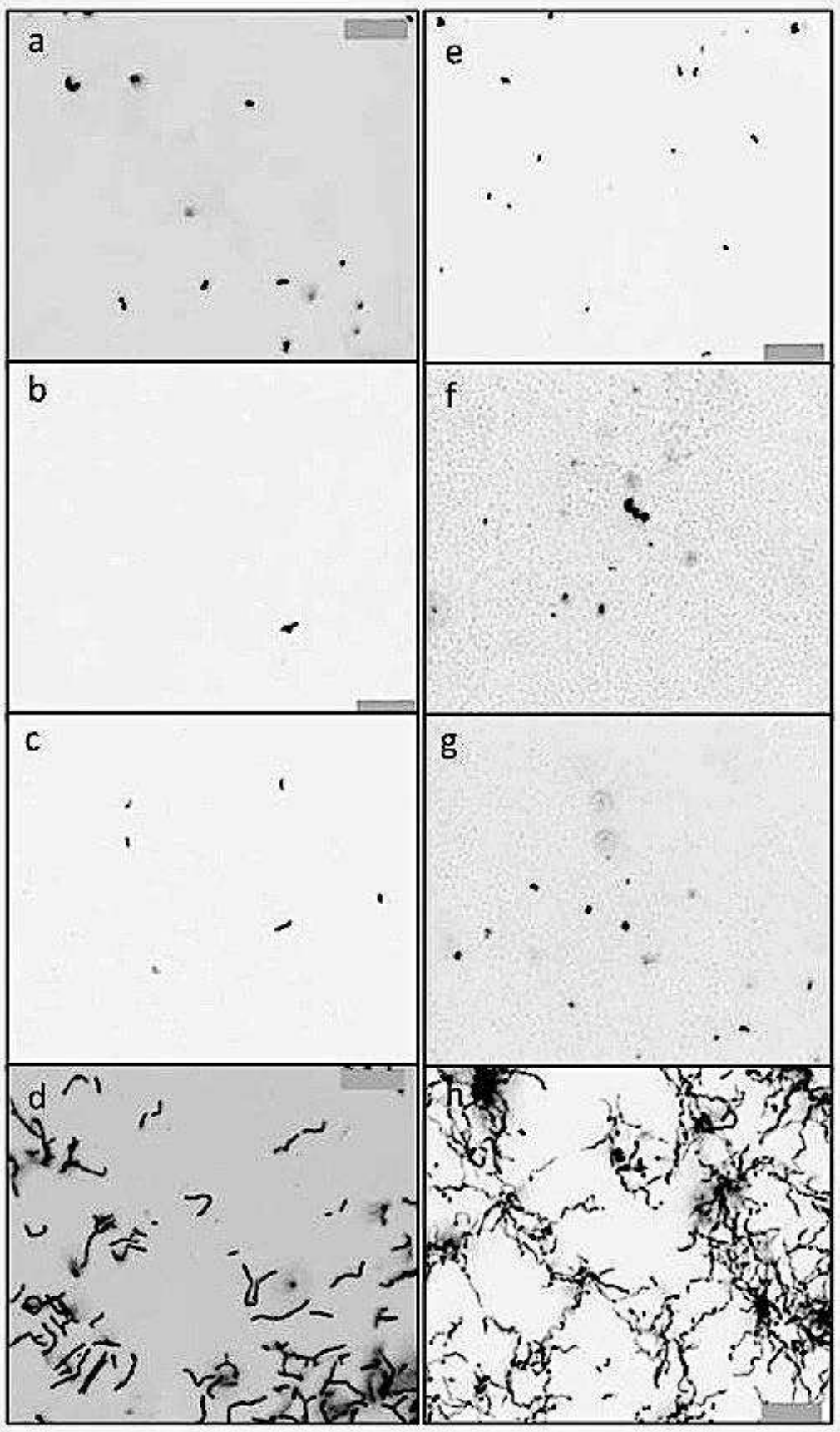

Figure 4

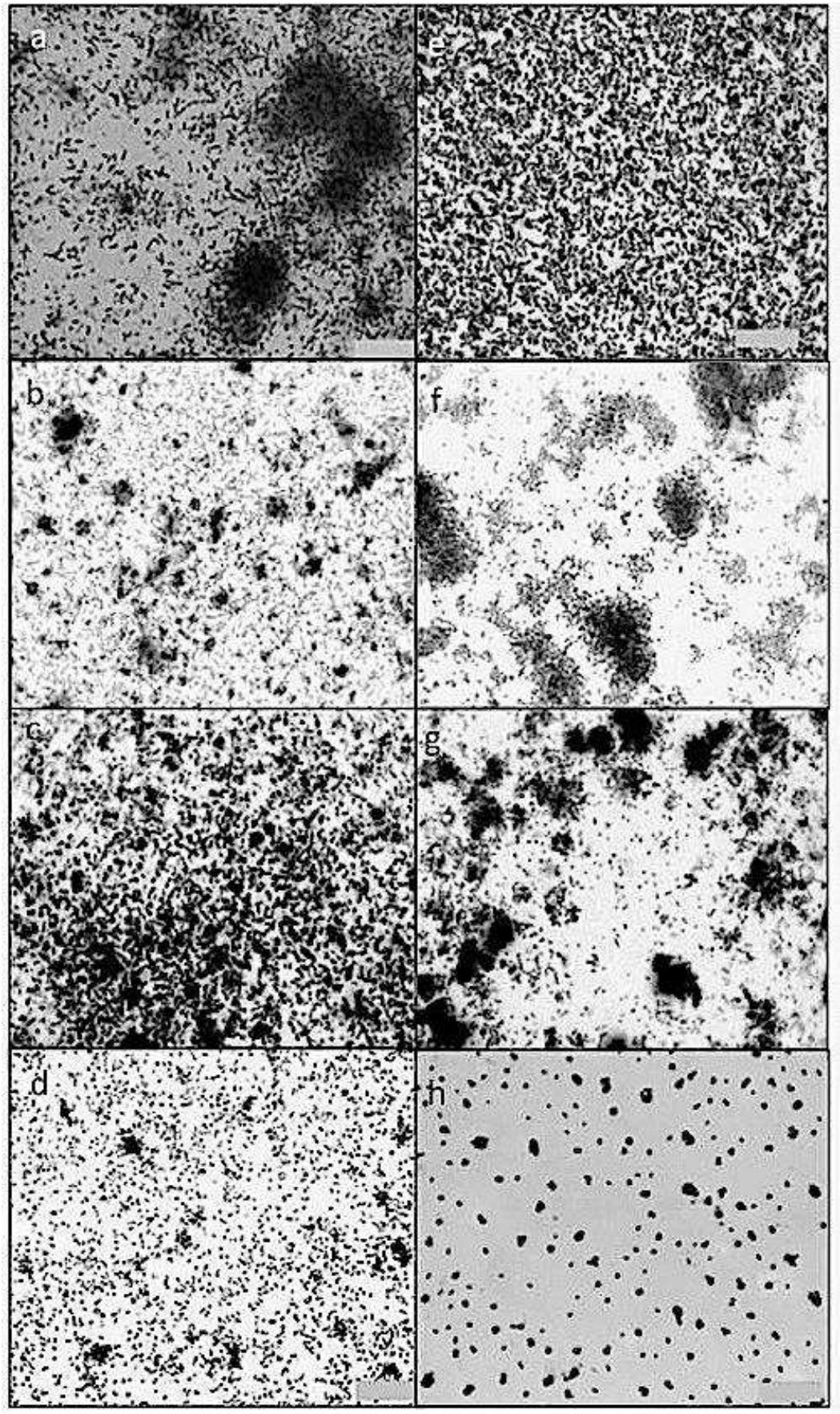

Figure 5

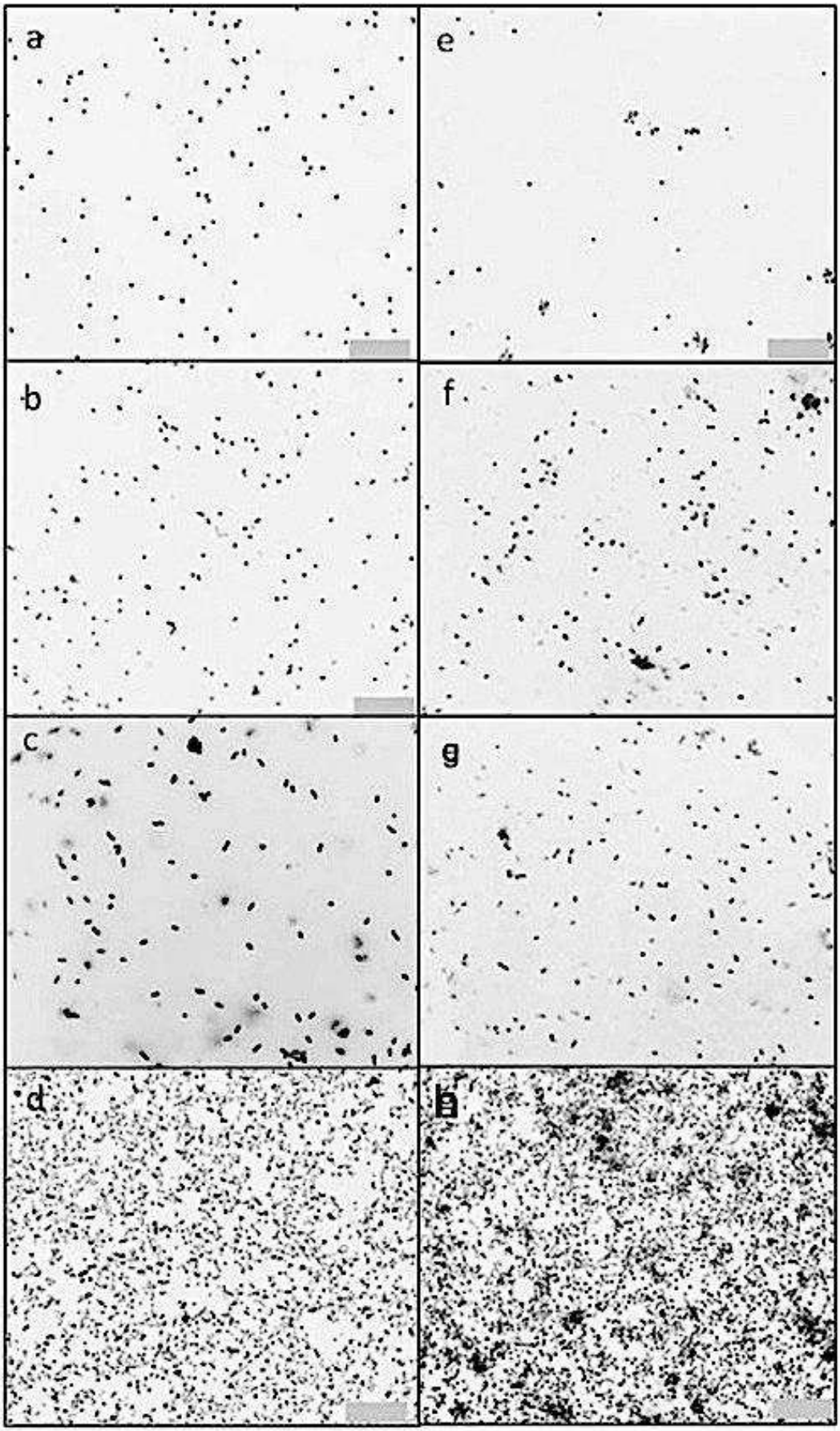

Figure 6

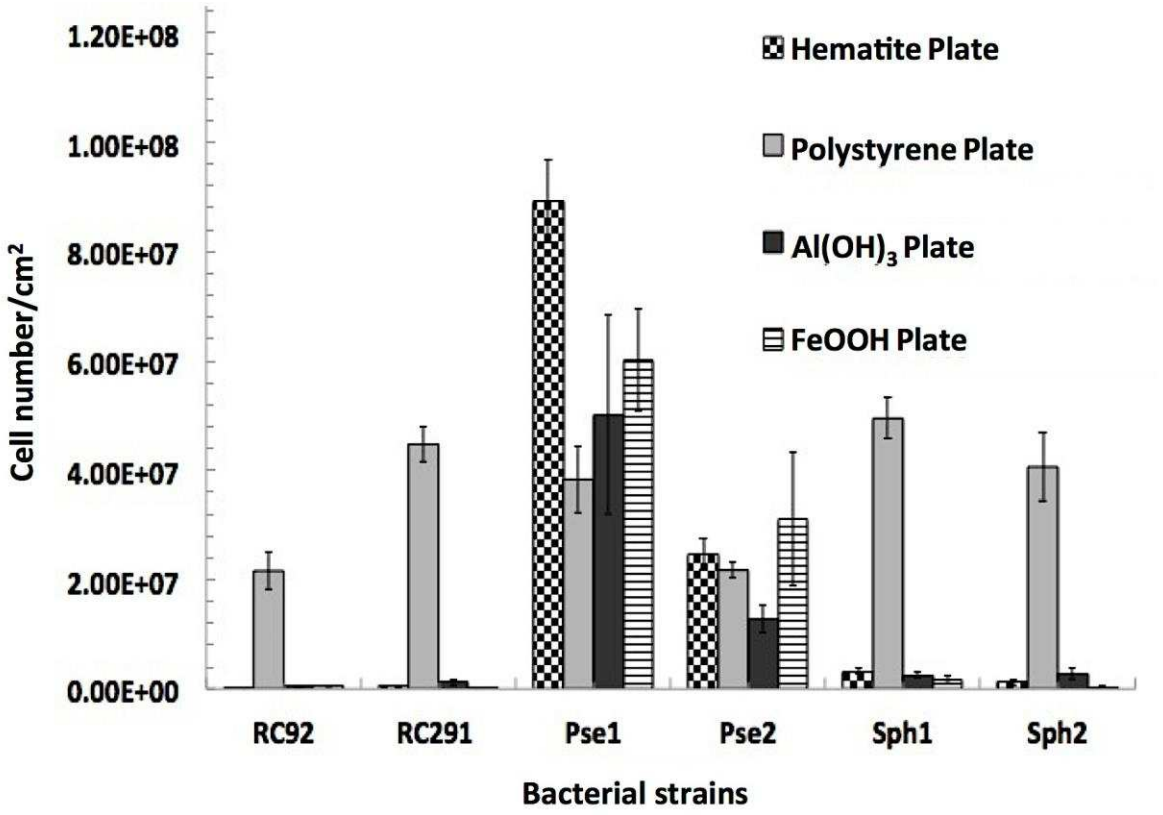
1.20E+08
1.00E+08
8.00E+07
6.00E+07
4.00E+07
2.00E+07
0.00E+00
Cell number/cm²
Hematite Plate
Polystyrene Plate
Al(OH)3 Plate
FeOOH Plate
RC92
RC291
Pse1
Pse2
Sph1
Sph2
Bacterial strains

Figure 7

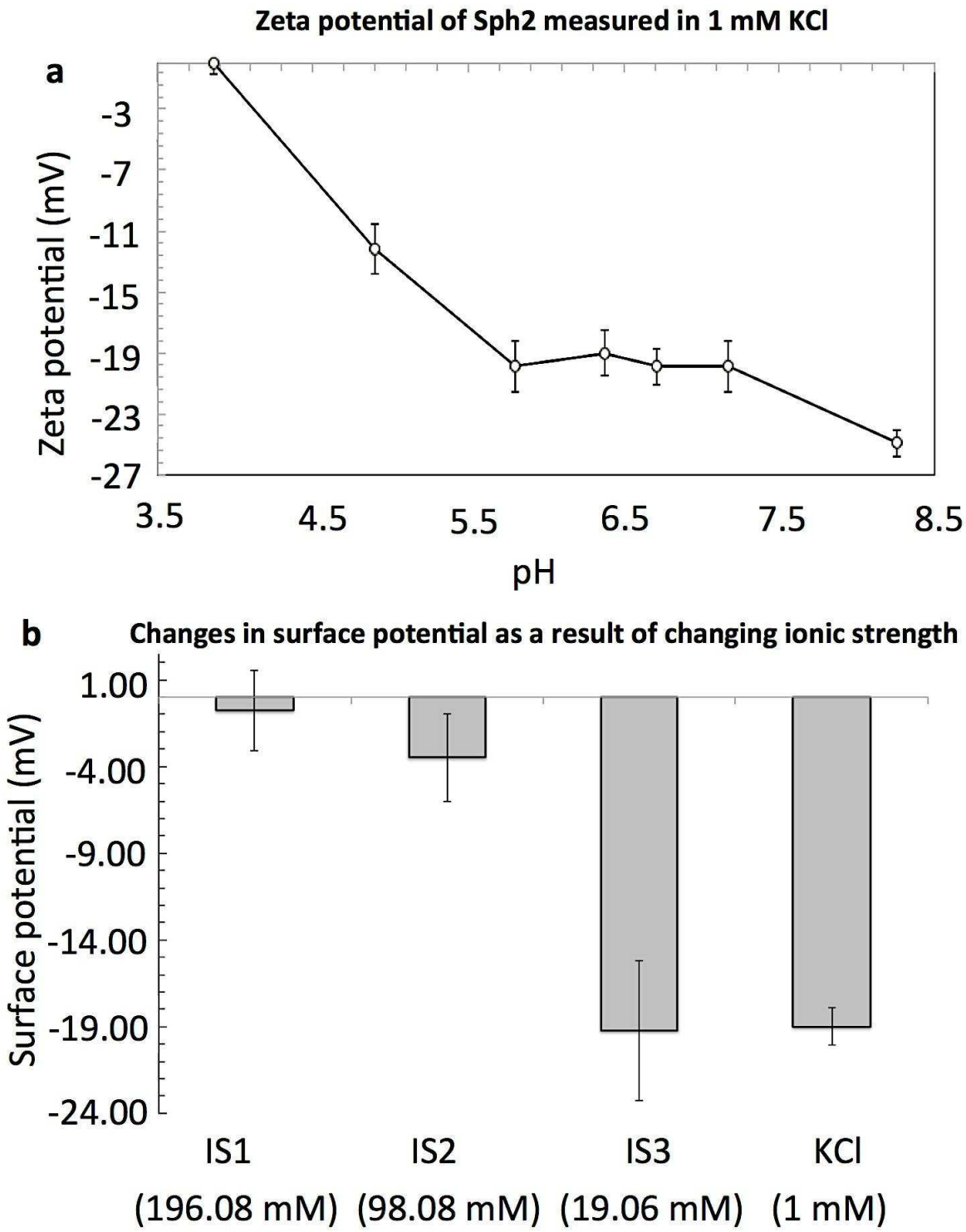
Zeta potential of Sph2 measured in 1 mM KCl
a
Zeta potential (mV)
-3
-7
-11
-15
-19
-23
-27
3.5
4.5
5.5
6.5
7.5
8.5
pH
b
Changes in surface potential as a result of changing ionic strength
Surface potential (mV)
1.00
-4.00
-9.00
-14.00
-19.00
-24.00
IS1
(196.08 mM)
IS2
(98.08 mM)
IS3
(19.06 mM)
KCl
(1 mM)

Figure 8

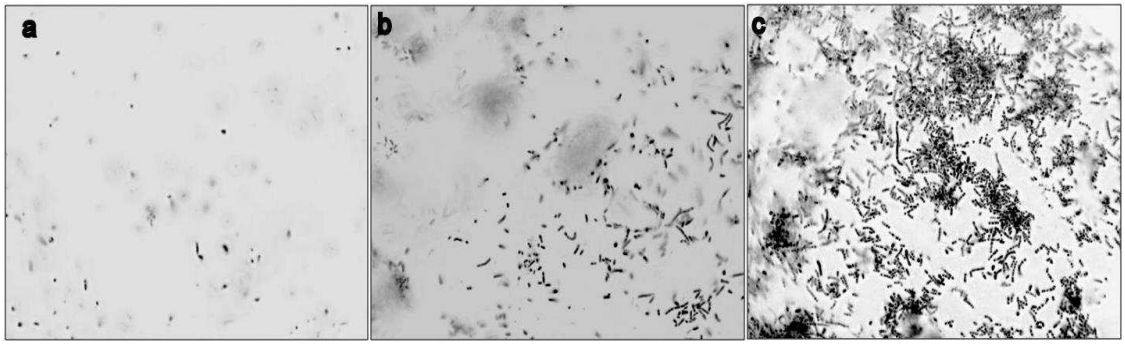

Figure 9

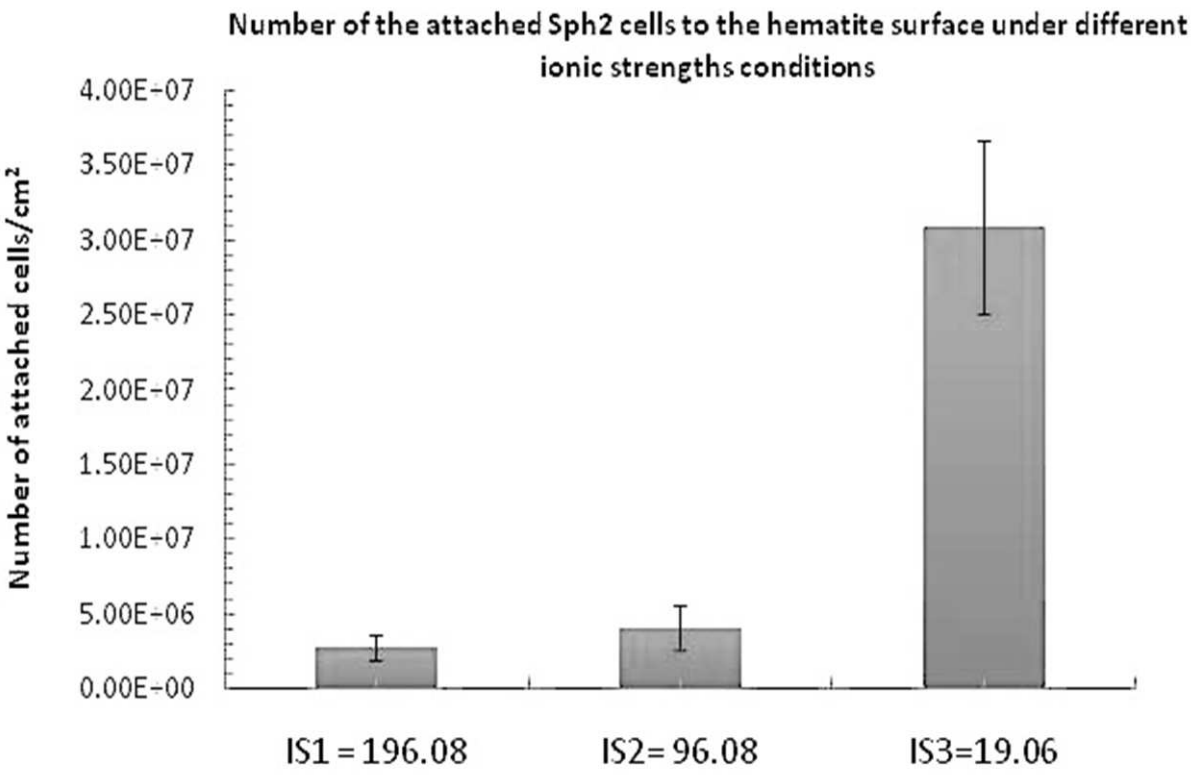

Figure 10

Table 1

Attachment Surface / Bacterial Strain	**Hematite Hydrophilic PZC=7.5**	**Goethite Hydrophilic PZC=8.5**	**Aluminum Hydroxide Hydrophilic PZC=8.9**	**Polystyrene Hydrophilic Neutral**
RC92 Hydrophobic, PZC<6.5	Negligible cell attachment	Negligible cell attachment	Negligible cell attachment	Dispersed chain-shape biofilm
RC291 Hydrophobic, PZC<6.5	Negligible cell attachment	Negligible cell attachment	Negligible cell attachment	Highly structured biofilm
Pse1 Hydrophilic, PZC<6.5	Extensive cell clusters	Extensive cell clusters	Extensive cell clusters	Sparse micro-colonies
Pse2 Hydrophilic, PZC<6.5	Extensive cell clusters	Extensive cell clusters	Extensive cell clusters	Sparse micro-colonies
Sph1 Hydrophobic, PZC<6.5	Poor, dispersed single-cell attachment	Poor, dispersed single-cell attachment	Poor, dispersed single-cell attachment	Extensive cell attachment
Sph2 Hydrophilic, PZC<6.5	Poor, dispersed single-cell attachment	Poor, dispersed single-cell attachment	Poor, dispersed single-cell attachment	Extensive cell attachment